Journal of Molecular Liquids 343 (2021) 117608

Contents lists available at ScienceDirect

Journal of Molecular Liquids

journal homepage: www.elsevier.com/locate/molliq

Quantum computational studies on optimization, donor-acceptor analysis and solvent effect on reactive sites, global descriptors, non-linear optical parameters of Methyl N-Boc-piperidine-3-carboxylate

M. Vimala [a], S. Stella Mary [a], R. Ramalakshmi [a], S. Muthu [b,*], R. Niranjana Devi [c], Ahmad Irfan [d]

[a] Department of Physics, St. Peter's Institute of Higher Education and Research, Avadi, Chennai 600054, India
[b] Department of Physics, Arignar Anna Govt. Arts College, Cheyyar, TamilNadu 604 407, India
[c] Department of Physics, Fatima college, Madurai, Tamilnadu 625018, India
[d] Department of Chemistry, College of Science, King Khalid University, P.O.Box 9004, Abha 61413, Saudi Arabia

ARTICLE INFO

Article history:
Received 25 August 2021
Revised 14 September 2021
Accepted 17 September 2021
Available online 22 September 2021

Keywords:
DFT
NBO
Solvent effect
FMO
Molecular docking

ABSTRACT

Methyl N-Boc-piperidine-3-carboxylate was examined by the computational calculation using the density functional theory. The optimized structure and molecular geometry of MBP3C were calculated. The topological properties such as electron density and the Laplacian of the electron density were calculated in the light of AIM theory. Donor-acceptor interactions were determined using the NBO analysis method. Solvents (water and ethanol) effect was analyzed in MEP, NLO, FMO, Mulliken charges and DOS. The electron density at bonding and antibonding sites was detected using ELF and LOL calculation. NCI analysis reveals the presence of weak Van der Waals interactions, hydrogen bonds and repulsive steric interactions in MBP3C. Molecular docking was done to found the best ligand–protein interactions of MBP3C.

1. Introduction

Piperidine is a nitrogen heterocyclic building block with $C_5H_{11}N$ as its molecular formula. It is a saturated aliphatic six-ring member with one amine bridge (–NH–) and 5 methylene bridges ($-CH_2$) [1]. Piper is a Latin word that means pepper [2]. Piperidine can be naturally procured from black pepper [3]. One of the most useful secondary Amine is piperidine. Ketones are converted into enamines using piperidine [4]. The enamines obtained from the piperidines can be utilized in the alkylation reaction [5]. It is extensively used as an admirable base for large scale deprotection of the Fmoc group from peptides in solid-phase peptide synthesis. It is an omnipresent building block and used as a synthetic indicator in the fusion of organic chemicals including pharmaceuticals [6,7]. Some of the piperidine derivatives used in pharmaceuticals are Minoxidil – for the treatment of male-pattern hair loss [8] and also an antihypertensive vasodilator [9], Haloperidol – for antipsychotic medication [10], Loperamide - to decrease the frequency of diarrhoea [11] and most importantly piperidine derivatives were explored as antiviral (anti-COVID19) which showed good inhibition [12].

DFT method is used to reveal the geometrical parameters, frontier orbital gap provides the knowledge of kinetic stability and chemical reactivity, donor–acceptor interactions, Fukui functions, reactive site analysis and electronic analysis [13–15].

The IUPAC name of Methyl N-Boc-piperidine-3-carboxylate [MBP3C] is 1-O-*tert*-butyl 3-O-methyl piperidine-1,3-dicarboxylate which has a molecular formula $C_{12}H_{21}NO_4$. Its molecular weight is 243.3 g/mol. MBP3C is a heterocyclic organic compound with one piperidine ring and two functional groups methyl and carboxylate. Carboxylates are the salts and esters of carboxylic acids. Carboxylate ions are resonance-stabilized. The Methyl group is very stable in most compounds and its reactivity depends on the adjacent substituents.

Literature survey confirms that the title compound Methyl N-Boc-piperidine-3-carboxylate [MBP3C] has not been published yet. It encouraged us to reveal the computational theoretical properties such as conformational analysis, molecular structure, NBO, non-covalent interaction in terms of RDG [16]. The biological property was found to determine the pharma logical property and molecular docking is done [17].

Solvents find tremendous utilization in many fields such as the chemical and pharmaceutical industries. Solvents can affect stability and reaction rates. Ethanol is an organic and versatile solvent. It

* Corresponding author.
E-mail address: mutgee@gmail.com (S. Muthu).

https://doi.org/10.1016/j.molliq.2021.117608
0167-7322/

Table 1
PES analysis of MBP3C.

No. of Conformations	Scan coordinate (°)	Total energy (Hartree)
1	−160.0001328	−820.6461768
2	−150.0001328	−820.6439027
3	−140.0001328	−820.6403826
4	−130.0001328	−820.6357324
5	−120.0001328	−820.6305708
6	−110.0001328	−820.62586
7	−100.0001328	−820.6219539
8	−90.00013279	−820.6190179
9	−80.00013279	−820.6173471
10	−70.00013279	−820.6382408
11	−60.00013279	−820.6413155
12	−50.00013279	−820.6439215
13	−40.00013279	−820.6459241
14	−30.00013279	−820.6472575
15	−20.00013279	−820.6478898
16	−10.00013279	−820.6478206
17	−0.000132787	−820.6508786
18	9.999867214	−820.6508332
19	19.99986721	−820.6504861
20	29.99986721	−820.6493689
21	39.99986721	−820.6473347
22	49.99986721	−820.6443895
23	59.99986721	−820.6406375
24	69.99986721	−820.6363056
25	79.99986721	−820.6317824
26	89.99986721	−820.6276061
27	99.99986721	−820.624366
28	109.9998672	−820.6226156
29	119.9998672	−820.6402461
30	129.9998672	−820.643457
31	139.9998672	−820.6462856
32	149.9998672	−820.6485097
33	159.9998672	−820.6499585
34	169.9998672	−820.6505337
35	179.9998672	−820.6502754
36	189.9998672	−820.6494551
37	199.9998672	−820.6479779

can dissolve both polar and non-polar substances. Water is a universal solvent but an inorganic solvent. Ethanol and water are chosen and their effect was observed in frontier orbital analysis, non-linear optical parameters, Mulliken charge, DOS and reactive site analysis of Methyl N-Boc-piperidine-3-carboxylate [MBP3C].

2. Computational details

The theoretical calculations have been performed at DFT/B3LYP method with basis set 6-311G++(d, p) using the Gaussian 09 W [18]. The optimized structure, geometric parameters (length and angle) of MBP3C were calculated. Mulliken charge arrangements, Fukui function, hyperpolarizability property, MEP analysis were visualized and HOMO-LUMO images, the bandgap energy in different phases was determined using GaussView5.0 [19]. NBO calculations were executed and the hyper conjugated interaction energies were computed by the second-order perturbation method [20]. The topological properties were calculated with the help of AIMALL software [21]. Using Multiwfn 3.6 [22] software ELF and LOL, NCI analysis was calculated for MBP3C. The bonding and antibonding of MBP3C was obtained using GaussSum2.2 software [23]. And molecular docking has been done using Auto dock 4.2 software [24].

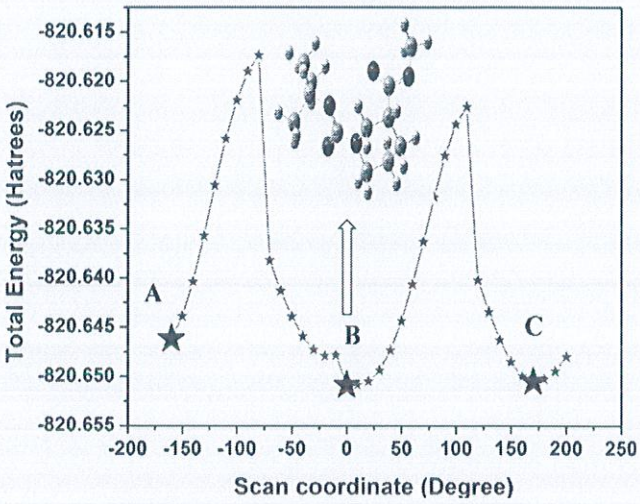

Fig. 1. Potential energy surface scan of MBP3C.

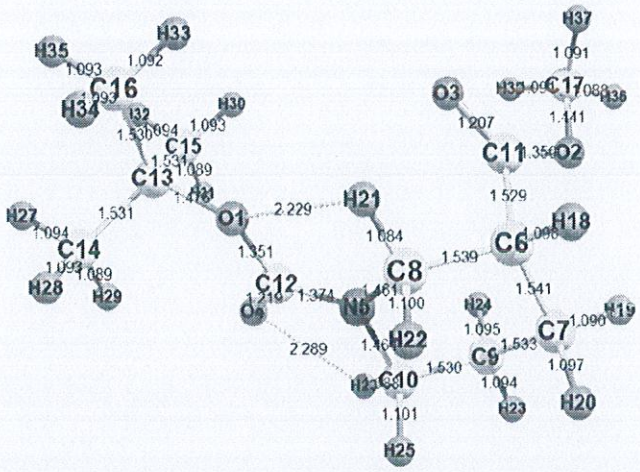

Fig. 2. Optimized geometric structure of MBP3C with atoms numbering.

3. Result and analysis

3.1. Conformational analysis

A cautious conformational analysis is done to MBP3C to find the least energy and stable conformers. The carbon atoms rotation about a single bond which results in atomic spatial arrangements within the organic compounds was studied by potential energy surface (PES) [25]. A relaxed PES scan was carried out to the dihedral angle C10-N5-C12-O1 and is rotated for 36 steps with 10° intervals from −180° to 180°. The scan coordinates with 37 energy conformations are listed in Table 1. The most stable conformers of MBP3C are at the saddle point −160°, −0.0001°, 170° with global minimum energy values −820.646, −820.651, −820.651 Hartree is shown in Fig. 1.

3.2. Optimized description

The atom numbering pattern with a bond length of MBP3C was found using GaussView5.0 and shown in Fig. 2. The optimized parameters such as distance between the atoms and bond angle

were calculated and compared with structurally related compounds [26] and tabulated in Table 2. From the tabulation it is found that the angle between C_{13}–O_1–H_{21} has the highest bond angle 146.8° and C_{12}–O_4–H_{26} has the least bond angle 83.9°. The bond length determines the properties of the atom such as atom size, bond energy and electronegativity. The bond distance is contrarily equal to the electronegativity and the bond energy. In MBP3C, O_4–H_{26} has the longest bond length 2.289 Å and C_8–H_{21} has the shortest bond length 1.08 Å which means, O_4–H_{26} has the least bond energy and electronegativity and C_8–H_{21} has the largest bond energy and electronegativity.

3.3. Natural bond orbital (NBO) analysis

NBO is nothing but an estimation of maximum electron density present in bonding orbital. It is also used to calculate the stability, charge transfer, basicity, reactivity and donor–acceptor interactions of the molecule [27,28]. NBOs are one of the arrays of natural

Table 2
Geometrical parameters optimized in MBP3C bond length (Å) and bond angle (°) with 6–311++G(d,p) basis set.

Bond length (Å)	Experiment [a]	B3LYP/6–311++G(d,p)	Bond Angle (°)	Experiment[a]	B3LYP/6–311++G(d,p)
O1-C12	1.3457	1.351	C8-N5-C10	114.27	116
O1-C13	1.4815	1.476	C8-N5-C12	124.88	124.1
O2-C11	1.3384	1.35	N5-C8-C6	110.43	111
O2-C17		1.441	N5-C8-H21	109.5	108.9
O3-C11	1.2303	1.207	N5-C8-H22	109.5	109.6
O4-C12	1.205	1.219	C10-N5-C12	114.27	118.6
N5-C8	1.4669	1.461	N5-C10-C9	110.43	110.7
N5-C10	1.463	1.464	N5-C10-H25	109.6	109.1
N5-C12	1.344	1.374	N5-C10-H26	109.5	107.8
C6-C7	1.512	1.541	C7-C6-C8	109.6	111
C6-C8	1.537	1.539	C7-C6-C11		114.7
C6-C11		1.529	C7-C6-H18	107.4	108.4
C6-H18	0.99	1.098	C6-C7-C9	109.6	111.3
C7-C9	1.512	1.533	C6-C7-H19		110.4
C7-H19	0.99	1.09	C6-C7-H20	107.4	107.7
C7-H20	0.99	1.097	C8-C6-C11		110.6
C8-H21	0.99	1.084	C8-C6-H18		107.3
C8-H22	0.99	1.1	C6-C8-H21	110.6	110.5
C9-C10	1.5317	1.53	C6-C8-H22	109.4	108.3
C9-H23	0.98	1.094	C11-C6-H18		104.3
C9-H24	0.98	1.095	C9-C7-H19		111
C10-H25	0.98	1.101	C9-C7-H20		109.1
C10-H26	0.98	1.088	C7-C9-C10		111.1
C13-C14	1.512	1.531	C7-C9-H23	109.4	110.1
C13-C15	1.512	1.531	C7-C9-H24	108	110
C13-C16		1.53	H19-C7-H20		107.1
C14-H27	0.98	1.094	H21-C8-H22	109.4	108.5
C14-H28	0.98	1.093	C8-H21-O1		102.9
C14-H29	0.98	1.089	C10-C9-H23	109.7	109.2
C15-H30	0.98	1.093	C10-C9-H24	109.4	109.2
C15-H31	0.98	1.089	C9-C10-H25	109.4	109.6
C15-H32	0.98	1.094	C9-C10-H26		111.7
C16-H33	0.98	1.092	H23-C9-H24	109.4	107
C16-H34	0.98	1.093	H25-C10-H26	109.5	107.8
C16-H35		1.093	C10-H26-O4	109.5	104.5
C17-H36		1.088	C14-C13-C15	108	112.5
C17-H37		1.091	C14-C13-C16	108	110.7
C17-H38		1.091	C13-C14-H27	109.5	109.4
O1-H21		2.229	C13-C14-H28	110.66	110.3
O4-H26		2.289	C13-C14-H29	111.09	111.2
			C15-C13-C16	109.5	110.6
Bond Angle		**B3LYP/6–311++G(d,p)**	C13-C15-H30		110.2
C12-O1-C13	121.57	121.5	C13-C15-H31	111.05	111.3
O1-C12-O4	124.04	124.9	C13-C15-H32	109.5	109.3
O1-C12-N5	111.74	111.4	C13-C16-H33	109.5	110.5
C12-O1-H21		89.9	C13-C16-H34	109.5	110.6
O1-C13-C14	110.31	110.1	C13-C16-H35		110
O1-C13-C15	109.63	110.1	H27-C14-H28	109.5	108
O1-C13-C16	101.56	102.3	H27-C14-H29	109.5	108.9
C13-O1-H21		146.8	H28-C14-H29	109.5	108.9
C11-O2-C17	114.27	115.9	H30-C15-H31	109.5	109.1
O2-C11-O3	122.99	122.8	H30-C15-H32	109.5	108.2
O2-C11-C6	111.72	112.2	H31-C15-H32	109.5	108.7
O2-C17-H36		105.5	H33-C16-H34	109.5	108.6
O2-C17-H37		110.4	H33-C16-H35		108.6
O2-C17-H38		110.4	H34-C16-H35		108.5
O3-C11-C6		124.9	H36-C17-H37		110.7
O4-C12-N5		123.6	H36-C17-H38		110.7
C12-O4-H26		83.9	H37-C17-H38		109.2

[a] Taken from Ref[23]

localized orbital sets. These natural localized sets lie between atomic orbitals (AO) and molecular orbitals (MO):

$$MO \leftarrow NLMO \leftarrow NBO \leftarrow NHO \leftarrow NAO \leftarrow AO$$

Where NLMO – natural localized molecular orbit, NHO – natural hybrid orbital, NAO- natural atomic orbital.

In computational chemistry, the localized orbitals are used to forecast the electron density distribution in atoms and bonds between the atoms. The NBO analysis is used to find the intra and intermolecular bonding between the molecules, bond interactions, stability and is also used to inspect the charge deportation or collective effect in the atomic organization [29]. The stabilization energy of the donor–acceptor was estimated and reported in Table 3. The NBO analysis shows the transformation of charge from the lone pair nitrogen LP1(N5) to anti bond σ*(O4–C12) has the greatest stabilization energy 57.33 kcal/mol. The stabilization energy (E2) associated with hyper conjugative interaction between the electron donors lone pair oxygens LP (2) [O2, O1, O3, O4] to acceptors π*(O3-C11), σ*(O4-C12), σ*(O2-C11), σ*(O1-C12) have the next highest stabilization energy 44.51, 38.91, 32.77 and 29.02 kcal/mol for MBP3C.

3.4. Topological properties

A great tool that is used to analyze the electron density and Laplacian electron density $\nabla^2\rho(r)$ is Bader's AIM theory [30]. Using AIM theory, the topology of the electron density is revealed by its gradient vector field. The topological properties of the charge density distribution are given in Table 4. The electron density $\rho_{BCP(r)}$ of the C-C bonds in the ring ranges from 1.616 e/Å^3– 1.677 e/Å^3. Among the O-C bonds, the O3-C11 bond has the highest charge density value 2.717 e/Å^3 which shows the double bond nature of the bond. The N5-C12 bond has a greater electron density value of 2.035 e/Å^3 than the remaining C-N bonds such as N5-C8 and N5-C10 which might be due to the bonding of the C12 atom with the two electronegative oxygen atoms O1 and O4.

Moreover, the Laplacian of the electron density is the most important properties at the bond critical point which is the sum of eigenvalues of the Hessian matrix (λ1, λ2, λ3) and (λ1-3) are the curvatures of the electron density. Interestingly three C-H bonds such as C14-H27, C14-H28 and C15-H32 are having the same Laplacian values −21.3 e/Å^5 at the critical point. The more negative shows the more concentration of electronic charges between the nuclei which further shows the share shell interaction. Among all the bonds, the O-H bonds such as O1-H21 and O4-H31 are having positive Laplacian values which portray the closed-shell interaction between the O and H atoms. Since the charges are concentrated in the internuclear region but spilt out of the atomic basin that paves way for the locally depleted electronic charge [31,32]. The sharing of charges in the covalent bonds present in the molecule is shown in Fig. 3. in which the lone pairs of O4 and O10 atoms are noticed.

The ellipticity of the bond is defined as, $\varepsilon = 1 - |\lambda_1/\lambda_2|$, where λ1 and λ2 are the principal curvatures of the electron density in the plane perpendicular to the bond (λ1 < λ2 < 0). It denotes the deviation from cylindrical symmetry at the BCP which helps to identify the pure σ bond from π character [33]. The bonds such as C9-H23 and C6-C7 are exhibiting their cylindrical symmetry due to their low ellipticity values of 0.003 and 0.004 respectively.

3.5. Electrostatic potential map (MEP)

From the optimized description of the MBP3C molecule, MEP's map and contour figure was obtained by using Gauss View 5.0 program in the gas phase and solvents (ethanol and water) phase are shown in Fig. 4. The colour coding in the picture was utilized to

Table 3
Second order perturbation theory of the Fock matrix NBO analysis of the MBP3C.

DonorNBO(i)	Type	ED/e	AcceptorNBO(j)	Type	ED/e	E(2)[a] kcal/mol a.u.	E(j)-E(i)[b] a.u.	F(i,j)[c] a.u.
C6-C11	σ	1.96972	O2-C17	σ*	0.01631	4.04	0.92	0.055
C6-H18	σ	1.95243	O3-C11	π*	0.21086	6.04	0.5	0.051
C6-H18	σ	1.95243	N5-C8	σ*	0.02662	3.62	0.84	0.05
C8-H21	σ	1.98025	N5-C10	σ*	0.02365	3.59	0.86	0.05
C9-H23	σ	1.97632	N5-C10	σ*	0.02365	3.5	0.85	0.049
C10-H26	σ	1.98018	N5-C8	σ*	0.02662	3.9	0.84	0.051
C14-H27	σ	1.98293	O1-C13	σ*	0.05711	4.61	0.77	0.054
C15-H32	σ	1.98268	O1-C13	σ*	0.05711	4.66	0.77	0.054
C16-H33	σ	1.98743	C13-C14	σ*	0.02995	3.62	0.88	0.051
C16-H34	σ	1.98754	C13-C15	σ*	0.02975	3.6	0.88	0.051
C16-H35	σ	1.9834	O1-C13	σ*	0.05711	4.75	0.79	0.055
O1	LP(1)	1.9553	O4-C12	π*	0.02506	7.69	1.12	0.083
O1	LP(2)	1.82817	O4-C12	σ*	0.36665	38.91	0.33	0.107
O1	LP(2)	1.82817	C13-C14	σ*	0.02995	4.66	0.7	0.053
O1	LP(2)	1.82817	C13-C15	σ*	0.02975	4.71	0.7	0.053
O2	LP(1)	1.96204	O3-C11	σ*	0.02356	8.33	1.16	0.088
O2	LP(2)	1.79916	O3-C11	π*	0.21086	44.51	0.34	0.11
O2	LP(2)	1.79916	C17-H37	σ*	0.01355	4.76	0.72	0.055
O2	LP(2)	1.79916	C17-H38	σ*	0.01345	4.79	0.72	0.055
O3	LP(2)	1.85084	O2-C11	σ*	0.1052	32.77	0.61	0.127
O3	LP(2)	1.85084	C6-C11	σ*	0.06454	16.11	0.66	0.094
O4	LP(2)	1.83941	O1-C12	σ*	0.09472	29.02	0.59	0.119
O4	LP(2)	1.83941	N5-C12	σ*	0.07831	21.9	0.67	0.11
N5	LP(1)	1.71895	O4-C12	σ*	0.36665	57.33	0.26	0.112
N5	LP(1)	1.71895	C6-C8	σ*	0.02437	4.09	0.61	0.048
N5	LP(1)	1.71895	C8-H22	σ*	0.02275	5.73	0.64	0.058
N5	LP(1)	1.71895	C9-C10	σ*	0.01842	4.07	0.63	0.049
N5	LP(1)	1.71895	C10-H25	σ*	0.0248	5.84	0.63	0.058

[a] E(2) means the energy of hyper conjugative interaction (stabilization energy).
[b] Energy difference between donor (i) and acceptor (j) NBO orbitals.
[c] F(i,j) is the Fock matrix element between i and j NBO orbitals.

Table 4
Topological properties of the molecule MBP3C.

Bonds	ρ (e/Å^3)	$\nabla^2\rho$(e/Å^5)	ε
-C7	1.616	−12.8	0.004
C6-C8	1.655	−13.6	0.030
C7-C9	1.635	−13.1	0.010
C9-C10	1.671	−13.9	0.030
C13-C14	1.674	−13.9	0.028
C13-C15	1.673	−13.9	0.028
C16-C13	1.677	−14.1	0.036
N5-C8	1.717	−15.5	0.055
N5-C10	1.734	−15.8	0.042
N5-C12	2.035	−20.6	0.242
O1-C12	1.969	−14.9	0.064
O1-C13	1.617	−7.73	0.034
O2-C11	1.962	−12.3	0.017
O2-C17	1.628	−8.07	0.015
O3-C11	2.717	−6.75	0.082
O4-C12	2.710	−10.8	0.110
C6-H18	1.845	−21.7	0.007
C7-H19	1.863	−22.2	0.010
C7-H20	1.841	−21.6	0.010
C8-H21	1.904	−23.4	0.022
C8-H22	1.871	−22.3	0.032
C9-H23	1.847	−21.9	0.003
C9-H24	1.848	−21.8	0.005
C10-H25	1.870	−22.4	0.033
C10-H26	1.898	−23.2	0.023
C14-H29	1.871	−22.3	0.013
C14-H27	1.824	−21.3	0.014
C14-H28	1.826	−21.3	0.014
C15-H30	1.832	−21.5	0.014
C15-H31	1.870	−22.3	0.014
C15-H32	1.823	−21.3	0.014
C16-H33	1.838	−21.6	0.008
C16-H34	1.836	−21.6	0.008
C16-H35	1.838	−21.7	0.010
C17-H37	1.897	−23.1	0.040
C17-H36	1.900	−23.4	0.042
C17-H38	1.897	−23.2	0.040
O1-H21	0.108	1.73	0.198
O4-H31	0.127	1.75	0.513

forecast the physiochemical property and charge distribution of MBP3C. And also used to conclude the molecular shape, size, reactive sites, charge density, positive, negative and neutral electrostatic potential via colour coding [34]. Visualization of molecular interactions and chemical reactivity of the molecule were identified using the colour code. The red colour indicates the strongest repulsion region, the blue colour indicates the strongest attraction region and the green colour insists the neutral region [35]. The colour cryptograph of MBP3C in the gas phase lies between − 5.544e-2 to + 5.544e-2 a.u., in ethanol lies between −6.736e-2 to 6.736e-2 and in water lies between −6.796e-2 to 6.796e-2 and the increasing order of potential is red, orange, yellow, green and blue. Both solvents have increased the electrostatic potential but water has the greatest potential value. The red colour around the oxygen atom shows the negative molecular electrostatic potential (electrophilic attack). The blue colour around hydrogen and carbon shows the positive molecular electrostatic potential (nucleophilic attack).

3.6. HOMO-LUMO analysis

The molecular orbital theory describes the electronic behaviour of the molecule with the help of the physical properties of nature on an atomic scale. This theory considers that the electrons are not attached to the bonds between atoms, but they are moving under the impact of the nuclei in the whole molecule with certain conditions of quantum which allows the electrons to follow, as long as they are in eigenstates permitted [36]. One of the applications of this theory is FMO theory which describes the interactions of frontier orbitals (HOMO-LUMO). The difference between the frontier orbital gives the bandgap energy. The bandgap energy can be utilized to declare the molecular strength and stability of the molecule [37] and also used to confirm the bioactivity and the molecular reactivity [38]. If the energy gap of the molecule increases the molecular reactivity decreases. According to Koopman's theorem, the HOMO and LUMO orbital values gives the ionization potential (I) and electron affinity (A) value as follows

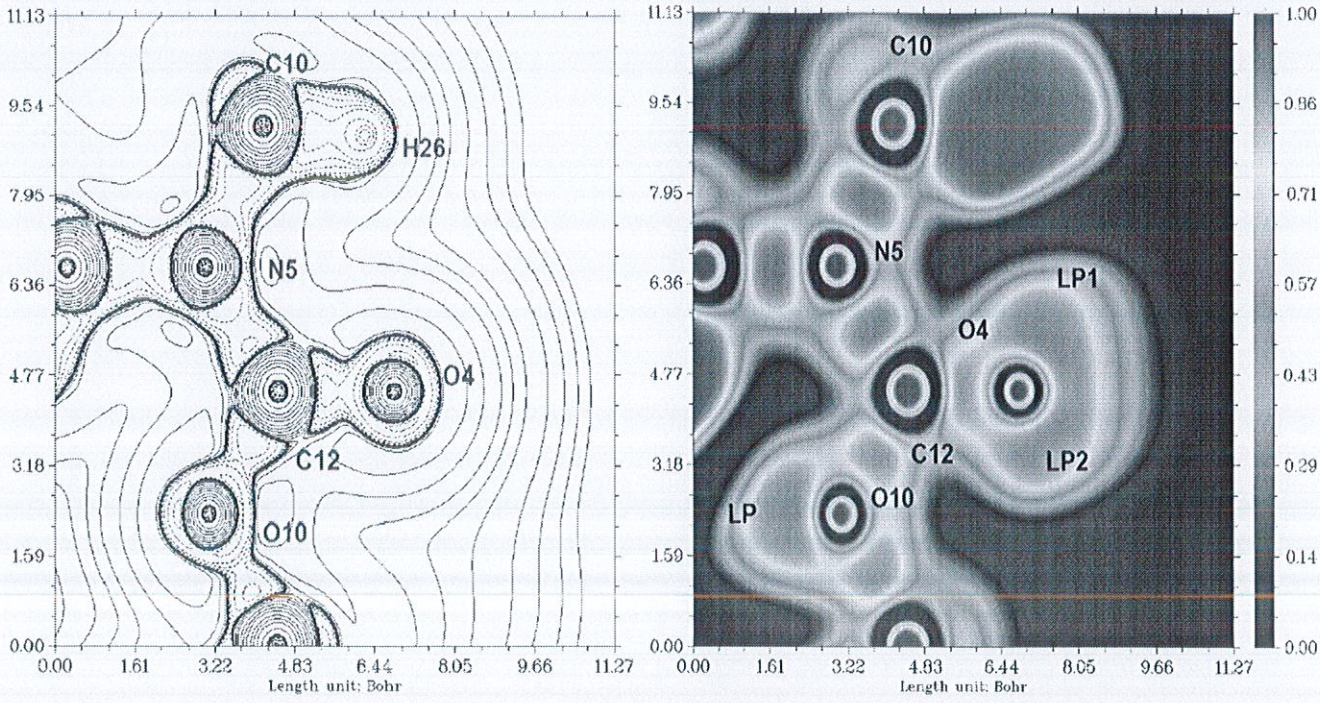

Fig. 3. a) Laplacian of electron density b) View of electron localization function of the molecule MBP3C.

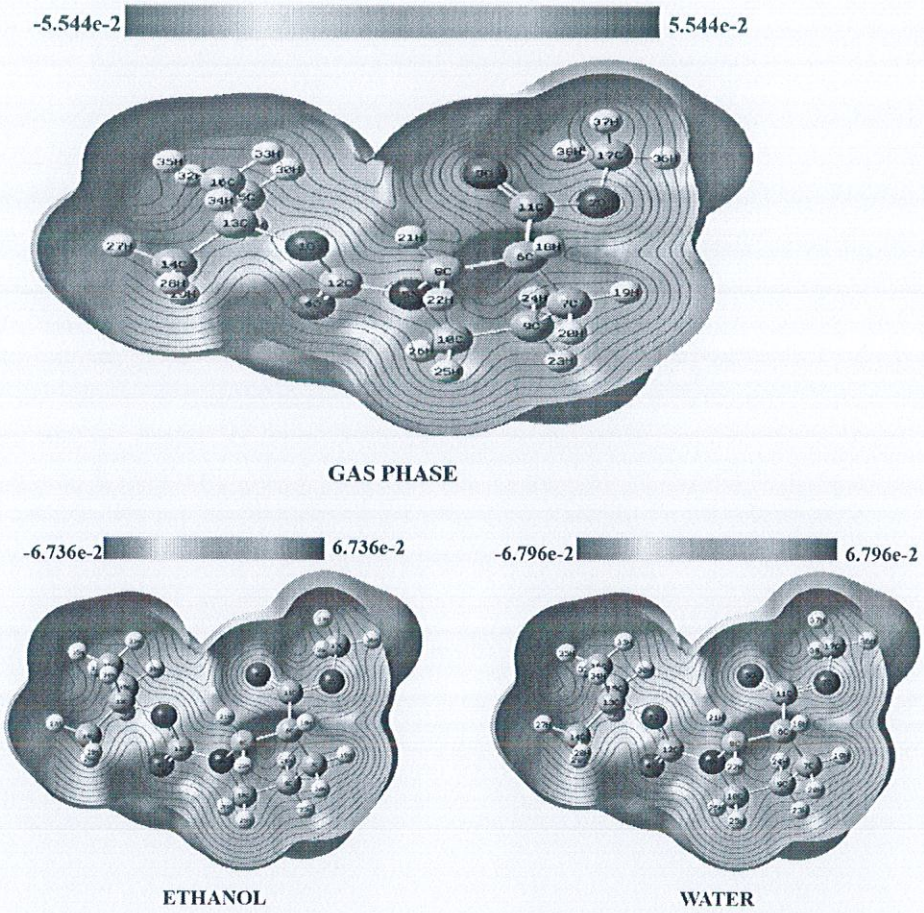

Fig. 4. Molecular Electrostatic Potential of MBP3C in gas phase and in solvent (water & ethanol) phase.

Table 5
Calculated global descriptors of MBP3C.

Global descriptors	GAS	ETHANOL	WATER
HOMO (eV)	−6.6039	−6.65078	−6.66112
LUMO (eV)	−0.5331	−0.53579	−0.53742
Ionization potential	6.6039	6.65078	6.66112
Electron affinity	0.5331	0.53579	0.53742
Energy gap (eV)	6.0708	6.11499	6.1237
Electronegativity	3.5685	3.593285	3.59927
Chemical potential	−3.5685	−3.59329	−3.59927
Chemical hardness	3.0354	3.057495	3.06185
Chemical softness	0.164723	0.163533	0.1633
Electrophilicity index	2.097614	2.111483	2.115509

$$I = -E_{HOMO}$$

$$A' = -E_{LUMO}$$

Electron affinity of the molecule gives the quantity of energy released during the formation of a negative ion (An electron attached to a neutral atom). Based on chemical potential, the electronegativity (χ), chemical hardness (η), molecule softness (σ), electrophilicity index (ω) [39] were calculated for MBP3C compound in the gas phase and solvents (ethanol and water) are listed in Table 5. The energy gap of MBP3C in the gas phase, ethanol and water is 6.0708 eV, 6.11499 eV and 6.1237 eV. Solvents increased the ionization potential, electron affinity, energy gap, electrophilicity, chemical potential and hardness of MBP3C. Solvents showed considerable changes in global descriptors. Among the solvents, the water showed the best result. Water has the following values HOMO −6–66112 eV, LUMO −0.53742 eV, energy gap 6.1237 eV, Ionization potential 6.66112 eV, electronegativity 3.59927, chemical hardness 3.06185 and electrophilicity index 2.115509. The Frontier molecular orbital for MBP3C in the gas phase and solvents is shown in Fig. 5.

3.7. Fukui function

The chemical reactivity of a compound is discussed in terms of the Hard-Soft Acid-Base theory (HSAB). By invoking the HSAB principle, one may establish the behaviour of the region concerning hard and soft reagents. The regions of a molecule where the Fukui function is large are chemically softer than the regions of a molecule where the Fukui function is small [40].

Fukui function is defined using a finite difference approximation

$$f+(r) = \rho N+1(r) - \rho N(r) \text{fornucleophilicattack}$$

$$f-(r) = \rho N(r) - \rho N-1(r) \text{forelectrophilicattack}$$

$$f0(r) = 1/2[\rho N+1(r) - \rho N-1(r)] \text{forradicalattack}$$

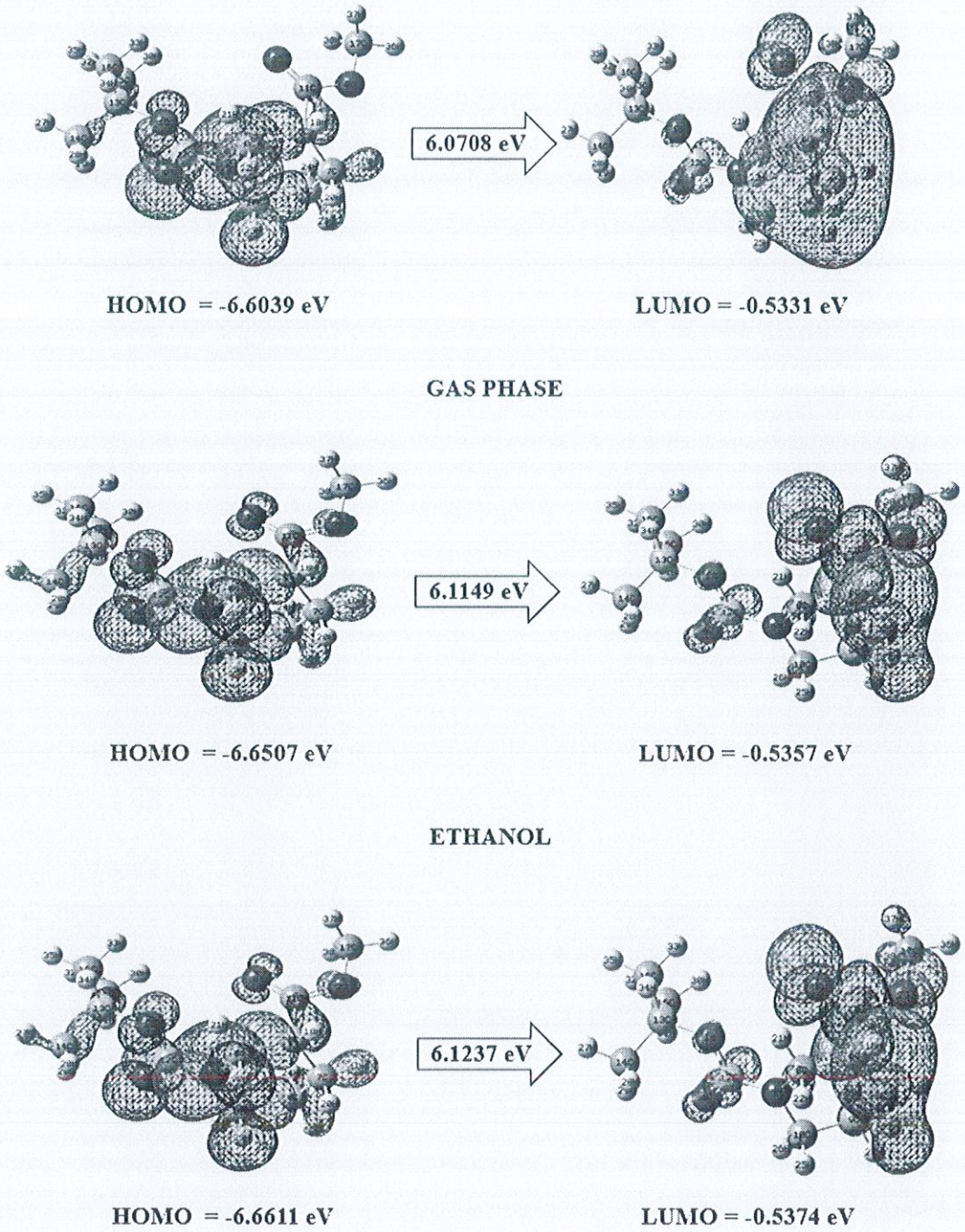

Fig. 5. Frontier molecular orbital for MBP3C in gas, water and ethanol.

here ρN - electron density at a point r in space around the molecule, N - electron number in the molecule, N + 1 - anion (An electron joined to LUMO of the neutral molecule), N-1 -cation (An electron extracted from the HOMO of the neutral molecule). Using the partitioning atomic charge scheme (Mulliken atomic population analysis), the values of Fukui functions are calculated as follows

$$f^{+}_{AK} = q_{AK}(N_A + 1) - q_{AK}(N_A)\text{fornucleophilicattack}$$

$$f^{-}_{AK} = q_{AK}(N_A) - q_{AK}(N_A - 1)\text{forelectrophilicattack}$$

$$f^{0}_{AK} = q_{AK}(N_A + 1) - q_{AK}(N_A - 1)\text{forradicalattack}$$

here $q_{AK}(N_A)$ - for N_A electrons the charge of Mulliken on atom k.

The Mulliken charge was found in a different phase and is shown in Table 6. Solvents showed mild changes in the Mulliken charges. The calculated Mulliken charges in the gas phase are from −0.66537 to 0.6185, in ethanol from −0.66766 to 0.63463 and in

Table 6
Mulliken charges of MBP3C in gas phase and solvent phase.

ATOMS	GAS	ETHANOL	WATER
1O	0.082892	0.053862	0.051838
2O	−0.06697	−0.08214	−0.08255
3O	−0.21579	−0.28387	−0.28804
4O	−0.24472	−0.31028	−0.31357
5 N	−0.03867	−0.03273	−0.03263
6C	0.618578	0.634638	0.636731
7C	−0.59854	−0.61126	−0.61207
8C	−0.66537	−0.66766	−0.66778
9C	−0.12601	−0.15023	−0.15051
10C	−0.31789	−0.31691	−0.3176
11C	−0.40454	−0.35448	−0.3519
12C	−0.1653	−0.14517	−0.14494
13C	0.063559	0.089179	0.090048
14C	−0.47799	−0.50088	−0.50217
15C	−0.41954	−0.42059	−0.41999
16C	−0.44491	−0.45487	−0.45467
17C	−0.20647	−0.22	−0.22076
18H	0.249838	0.27956	0.281229
19H	0.178182	0.179092	0.179026
20H	0.153962	0.168413	0.169384
21H	0.229752	0.224452	0.224001
22H	0.175646	0.200021	0.201632
23H	0.191127	0.205751	0.206542
24H	0.162046	0.161523	0.160979
25H	0.149048	0.168318	0.169541
26H	0.20496	0.191564	0.190669
27H	0.153511	0.167623	0.16857
28H	0.146497	0.15864	0.159434
29H	0.184843	0.172493	0.171766
30H	0.154164	0.146876	0.145888
31H	0.184386	0.175168	0.174724
32H	0.152275	0.169258	0.170509
33H	0.160703	0.159628	0.159086
34H	0.149801	0.158328	0.158966
35H	0.142506	0.158506	0.159556
36H	0.153851	0.167905	0.168598
37H	0.173195	0.177872	0.178042
38H	0.177384	0.182385	0.182433

water from −0.66778 to 0.63673. The complete knowledge of the molecule's reactive area was achieved by applying the Mulliken population analysis to get the Fukui functions [41] and dual descriptors[Δf] and tabulated in Table 7. In the gas phase, atom H18 possess −0.98896 the greater negative dual descriptor which means that the atom has a more electrophilic attack. The electrophilic attack of MBP3C lies in the order H18 > C6 > H 36 > H22 > H23 > C13 > H20 > H38 > H37 > C9 > H19 > H34 > - H25 > H33 > H32 > H29 > O2 > H35 > H28 > H26 > H31 > H27 > 03. The atom C17 acquires the maximum positive dual descriptor 1.53273 which means that the atom has a nucleophilic attack. The relative capability of nucleophilic attack is C7 > C17 > C8 > C11 > C10 > C16 > O4 > N5 > C15 > C14 > C12 > O1 > H21 > H30 > H24.

3.8. Hyperpolarizability property

Non-Linear Optical (NLO) components are used in data storage technology, optical communication, signal processing and laser technology. The important parameters to identify the NLO materials are polarizability(α) and first-order hyperpolarization(β) [42]. Such parameters are obtained by the theoretical computational DFT method. The dipole moment(D), polarizability(α) and first-order hyperpolarizability(β) values of MBP3C were analyzed and given in Table 8. For MBP3C the calculated dipole moment(D), polarizability(α) and first-order hyperpolarizability(β) are in gas phase 1.5281 D,4.8540 x10^{-23}esu and 1.3499 x10^{-30}esu, in ethanol 1.9587 D, 5.9552 x10^{-23}esu and 1.9004 x10^{-30}esu, in water 1.9822 D, 6.0113 x10^{-23}esu and 1.9223 x10^{-30}esu. In the gas phase, MBP3C possess 1.45 times greater hyperpolarizability than prototypical urea which ascertains that the title compound has good NLO property. Due to the solvents, there is a gradual increase in the computed NLO parameters with an increase in the dielectric constant of the solvents. Water showed the best hyperpolarizability value of 1.9223x10^{-30} esu which is 1.67 times the urea.

3.9. PDOS spectrum

Using Gauss sum software, the Density of energy state spectrum has been drawn in the gas phase and solvent phase are shown in Fig. 6a. DOS spectrum is used to analyze the electronic property [43]. HOMO- LUMO difference measures the electron conductivity. The HOMO-LUMO values and energy gap values of MBP3C are in gas phase (-6.44 eV, −0.47 eV, 5.97 eV), in ethanol (-6.6 eV, −0.44 eV, 6.16 eV) and in water (-6.61 eV, −0.44 eV, 6.17 eV). Fig. 6b partial density of state shows the molecular orbitals of the specified groups. Blue for C-H, green for C = C, red for C-C, pale blue for C-O, pink for C-N, yellow for unoccupied orbitals and black for virtual orbitals respectively. The bandgap of the molecule reveals the influence of one atom on the other atom which was noticed in the electronic transitions and NLO property of the molecule.

3.10. ELF and LOL analyses

Electron Localization Function (ELF) and Localized Orbital Locator (LOL) are the surface analysis that completely depends on the covalent bonds. It explains the molecular surface having the possibility to determine the electron pair [44]. ELF and LOL are similar because both depend on kinetic energy density. From the electron density pair, the ELF originates and LOL admits the maximized gradient of the localized orbitals when localized orbitals overlap [45]. The Colour shade map of MBP3C has been drawn using Multiwfn software and shown in Fig. 7a (ELF) and 7b (LOL). ELF colour map is plotted between the range 0.0–1.0. The localized electrons (bonded, nonbonded) were in the range of 0.5 – 1 and free electrons (delocalized electron) was predicted in the range < 0.5. If the electron Localization influences the electron density, then the LOL achieves high value i.e., > 0.5. ELF is established by considering the electron pair density of the molecule. High localization of electron occurs in a region because of the covalent bond existence or nuclear shell in that region [46]. From the ELF colour map, it is evident that the high localized bonded and nonbonded electrons are found around hydrogen atoms indicated by red colour. Delocalized electron is present around few Oxygens, Nitrogen and Carbon atoms are shown by blue regions. LOL map is plotted between the range 0 to 0.8. If the region possesses high electron density beyond the limit of the LOL map that region occurs white colour. At the centre of the hydrogen atom white colour appears which means the electronic density is higher than the colour scale limit of 0.8.Fig. 8.

3.11. Non-covalent index (NCI) analysis

The other name for non-covalent interaction is Reduced density gradient (RDG), which is a very fashionable technique to analyze weak interaction. Non-covalent interaction plays a key role in several chemical fields and biological systems because molecular analysis is unable to identify the complex noncovalent interaction in the design of new materials and drugs. Non-covalent interaction is a graphical representation that depends on the density of electrons (ρ) and the gradient of reduced density (s). It provides a broad knowledge to distinguish the weak van der Waals interactions, interactions of hydrogen bonds and repulsive steric interac-

Table 7
Condensed Fukui function for MBP3C.

	Mulliken atomic charges			Fukui functions			local softness			Dual descriptor
	0, 1 (N)	N + 1 (-1, 2)	N-1 (1,2)	fr +	fr -	fr 0	sr+ fr+	sr-fr-	sr0 fr0	Δfr = fr+ - fr-
1O	0.0829	0.0994	0.1214	0.0165	−0.0386	−0.0110	0.0034	−0.0081	−0.0023	0.0550
2O	−0.0670	−0.1206	−0.0622	−0.0536	−0.0048	−0.0292	−0.0112	−0.0010	−0.0061	−0.0488
3O	−0.2158	−0.2607	−0.1755	−0.0449	−0.0403	−0.0426	−0.0094	−0.0084	−0.0089	−0.0046
4O	−0.2447	−0.2648	−0.1003	−0.0201	−0.1445	−0.0823	−0.0042	−0.0302	−0.0172	0.1244
5 N	−0.0387	−0.0143	0.1298	0.0244	−0.1685	−0.0720	0.0051	−0.0352	−0.0151	0.1929
6C	0.6186	−0.2294	0.6192	−0.8479	−0.0006	−0.4243	−0.1773	−0.0001	−0.0887	−0.8473
7C	−0.5985	0.9653	−0.6296	1.5638	0.0311	0.7975	0.3270	0.0065	0.1668	1.5327
8C	−0.6654	0.3211	−0.7291	0.9865	0.0637	0.5251	0.2063	0.0133	0.1098	0.9228
9C	−0.1260	−0.3599	−0.1823	−0.2339	0.0563	−0.0888	−0.0489	0.0118	−0.0186	−0.2903
10C	−0.3179	0.1026	−0.3406	0.4205	0.0227	0.2216	0.0879	0.0048	0.0463	0.3978
11C	−0.4045	0.2184	−0.3685	0.6230	−0.0360	0.2935	0.1303	−0.0075	0.0614	0.6590
12C	−0.1653	−0.0692	−0.1819	0.0961	0.0166	0.0564	0.0201	0.0035	0.0118	0.0795
13C	0.0636	−0.1806	−0.0721	−0.2442	0.1357	−0.0542	−0.0511	0.0284	−0.0113	−0.3799
14C	−0.4780	−0.3188	−0.4609	0.1592	−0.0171	0.0711	0.0333	−0.0036	0.0149	0.1763
15C	−0.4195	−0.2408	−0.4097	0.1788	−0.0099	0.0844	0.0374	−0.0021	0.0177	0.1886
16C	−0.4449	−0.1275	−0.3963	0.3174	−0.0486	0.1344	0.0664	−0.0102	0.0281	0.3660
17C	−0.2065	0.9637	−0.2074	1.1701	0.0009	0.5855	0.2447	0.0002	0.1224	1.1693
18H	0.2498	−0.8045	0.3152	−1.0543	−0.0654	−0.5599	−0.2205	−0.0137	−0.1171	−0.9890
19H	0.1782	−0.0798	0.2278	−0.2580	−0.0496	−0.1538	−0.0539	−0.0104	−0.0322	−0.2084
20H	0.1540	−0.2623	0.1952	−0.4162	−0.0412	−0.2287	−0.0870	−0.0086	−0.0478	−0.3750
21H	0.2298	0.2200	0.2899	−0.0098	−0.0602	−0.0350	−0.0020	−0.0126	−0.0073	0.0504
22H	0.1756	−0.4978	0.2620	−0.6734	−0.0864	−0.3799	−0.1408	−0.0181	−0.0794	−0.5871
23H	0.1911	−0.2921	0.2581	−0.4832	−0.0670	−0.2751	−0.1010	−0.0140	−0.0575	−0.4162
24H	0.1620	0.1346	0.2077	−0.0274	−0.0457	−0.0366	−0.0057	−0.0096	−0.0076	0.0182
25H	0.1490	−0.0683	0.2431	−0.2173	−0.0941	−0.1557	−0.0454	−0.0197	−0.0326	−0.1232
26H	0.2050	0.1309	0.2564	−0.0740	−0.0514	−0.0627	−0.0155	−0.0107	−0.0131	−0.0226
27H	0.1535	0.0900	0.1986	−0.0635	−0.0451	−0.0543	−0.0133	−0.0094	−0.0114	−0.0185
28H	0.1465	0.1023	0.1638	−0.0442	−0.0173	−0.0308	−0.0092	−0.0036	−0.0064	−0.0268
29H	0.1848	0.1358	0.1929	−0.0491	−0.0081	−0.0286	−0.0103	−0.0017	−0.0060	−0.0410
30H	0.1542	0.1733	0.1689	0.0191	−0.0148	0.0022	0.0040	−0.0031	0.0005	0.0338
31H	0.1844	0.1539	0.1928	−0.0305	−0.0084	−0.0195	−0.0064	−0.0018	−0.0041	−0.0221
32H	0.1523	0.0585	0.1981	−0.0937	−0.0458	−0.0698	−0.0196	−0.0096	−0.0146	−0.0479
33H	0.1607	0.0418	0.1754	−0.1189	−0.0147	−0.0668	−0.0249	−0.0031	−0.0140	−0.1042
34H	0.1498	0.0095	0.1676	−0.1403	−0.0178	−0.0791	−0.0293	−0.0037	−0.0165	−0.1226
35H	0.1425	0.0807	0.1722	−0.0618	−0.0297	−0.0458	−0.0129	−0.0062	−0.0096	−0.0321
36H	0.1539	−0.5002	0.1836	−0.6540	−0.0298	−0.3419	−0.1368	−0.0062	−0.0715	−0.6242
37H	0.1732	−0.1482	0.1908	−0.3213	−0.0176	−0.1695	−0.0672	−0.0037	−0.0354	−0.3037
38H	0.1774	−0.1622	0.1857	−0.3396	−0.0084	−0.1740	−0.0710	−0.0017	−0.0364	−0.3313

Table 8
The values of calculated dipole moment μ(D), polarizability(α_o), first order hyperpolarizability (β_{tot}) components of MBP3C.

Parameters	GAS	ETHANOL	WATER
μx	−1.3965272	−1.7364542	−1.7522896
μy	0.2151968	0.1824696	0.1759444
μz	−0.5817555	−0.8876335	−0.9096626
μ(D)	1.5280829	1.95868874	1.98216077
αxx	187.629763	231.106596	233.359361
αxy	6.8876583	9.0958552	9.1583659
αyy	159.186559	205.45301	208.304406
αxz	2.4200253	6.3541236	6.6135508
αyz	1.2453945	0.9091442	0.9476045
αzz	140.907343	190.91946	194.602499
α (a.u)	162.574555	209.159689	212.088755
α (e.s.u)	2.4094E-23	3.0997E-23	3.1432E-23
Δα (a.u)	327.532973	401.836962	405.621212
Δα (e.s.u)	4.854E-23	5.9552E-23	6.0113E-23
βxxx	154.534229	305.228098	312.963137
βxxy	48.17457	94.1386195	97.1886738
βxyy	−69.101221	−82.3601529	−83.202003
βyyy	−50.783398	−72.8815685	−73.470913
βzxx	10.1386907	64.5806086	69.1152063
βxyz	17.2323098	40.8230801	42.1124593
βzyy	−13.498287	2.8167986	3.2200481
βxzz	−44.945124	−60.3231395	−61.261606
βyzz	−29.864624	−72.2326034	−75.495665
βzzz	−144.02019	−206.562556	−208.11038
βtot (a.u)	156.251705	219.968769	222.503767
βtot (e.s.u)	1.3499E-30	1.9004E-30	1.9223E-30

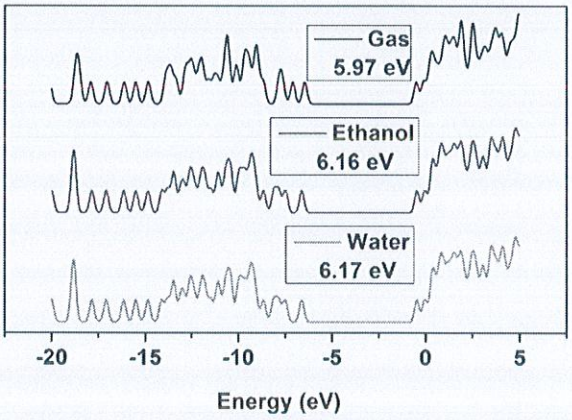

Fig. 6. a DOS spectra of MBP3C in gas and solvent phase with energy gap, b PDOS of MBP3C.

tions in miniature, complex molecules like proteins or DNA and solids [47]. Using Multiwfn software, scatter graph and colour-filled RDG isosurface of MBP3C with the help of VMD software was drawn and shown in figure (8a & b). The red colour at the centre of the piperidine ring shows the strong steric effect and the green colour shows the weak van der Waal interactions. The scat-

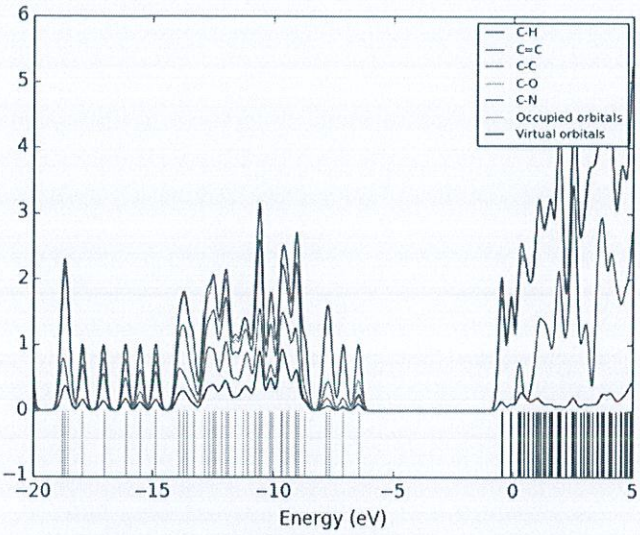

Fig. 6 (*continued*)

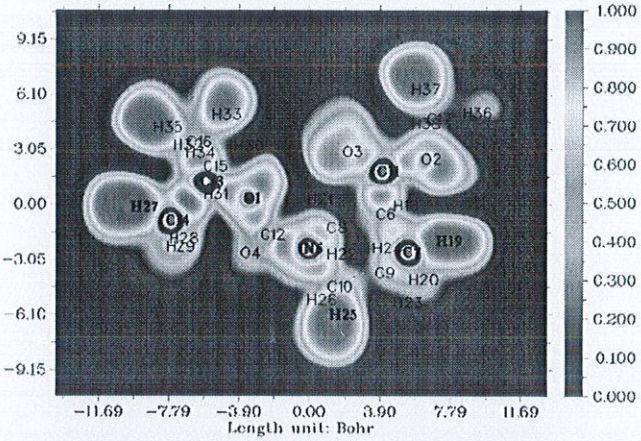

Fig. 7. a ELF colour filled map of MBP3C, b LOL colour filled of MBP3C.

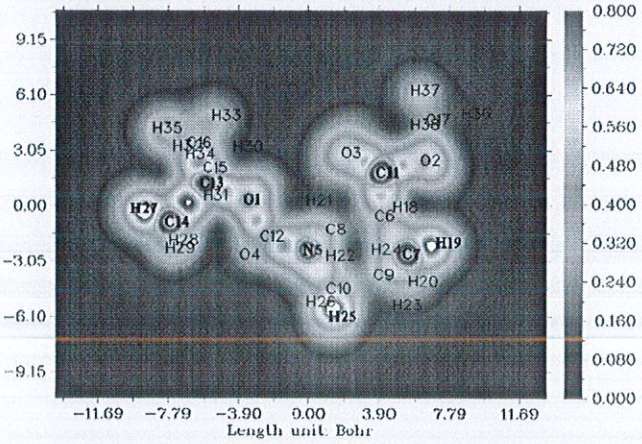

Fig. 7 (*continued*)

ter graph was drawn between the RDG and sign (λ_2) ρ. The sign (λ_2) ρ values are useful to forecast the interaction nature, if sign (λ_2) $\rho > 0$ then it will be the repulsive interaction and for sign (λ_2) $\rho < 0$ then it will be the attractive interaction. The spikes in the scatter graph can be classified into three types and were marked by blue, green and red circles. The blue circle indicates the H-bond(attractive), green indicates the vdW interactions and red indicates the steric effect(repulsive) of MBP3C.

3.12. Druglikeness

Drug likeness is a subjective approach used in designing drugs concerning the aspects like bioavailability. Drug likeness study is carried out with the molecular structure, no need for the substance to be prepared and tested. A universal technique to analyze drug-likeness is the Five Rule of Lipinski's, which envelopes the hydrophilic group number, molar refractivity and bioavailability score. The estimations are based on several rules such as Ghose Filter rule, Lipinski's rule, rule of BBB, CMC-50, MDDR like, Veber rule and QED [48]. Hydrogen bond donors (HBD) and acceptors (HBA), bioavailability score, Molar refractivity (MR), Number of rotatable bonds, Topological Polar Surface Area (TPSA), and log kp are the essential ADME parameters to determine the drug-likeness property of any molecule. These parameters of MBP3C were calculated and presented in Table 9. MBP3C has zero hydrogen bond donor, four hydrogen bond acceptors and molar refractivity 67.49. MBP3C satisfied Lipinski's five rules.

3.13. Ramachandran plot

The Ramachandran plot is used to visualize energetically active regions for a polypeptide backbone torsion angle psi (ψ) against phi (φ) of amino acid residues present in the protein [49]. Using this plot one can get the idea of the protein's secondary structure. The graph is plotted between amino acid residue's dihedral angles ψ against φ in protein structure. This plot was established by G.N. Ramachandran, et.al in the year 1963 by plotting the graph between the φ values in the x-axis and the ψ values in the y-axis [50]. Using PROCHECK server Ramachandran plot was drawn and shown in Fig. 9. Each black dot on the graph represents each amino acid. the red region represents the allowed regions where there are no steric clashes. The allowed regions have alpha-helical and beta-sheet conformations. The cluster of dots present in the map shows that the protein has a right-handed α helix secondary structure. Protein 2ACE [51] is a serine hydrolase that has 527 residues and 87.2% of the residues lies in the most favoured region. Protein 5RH0 [52] is a hydrolase inhibitor that has 304 residues and 89% of the residues are lying in the most favoured region. 6Y9B [53] is a membrane protein that has 244 residues and 92.3% lies in the most favoured region. The percentage of the residue in the most favoured, additional allowed, generally granted and forbidden regions were presented in Table 10.

3.14. Molecular docking

As biological research has been increased, it needs informatics tools. For example, drug discovery research requires the screening of many compounds for an appropriate protein target. Important tools that can intensify such screening are molecular docking and database mining [54]. Molecular docking is a tool used for drug discovery, due to its ability to predict the binding-frame work of miniature molecule ligands to the suitable target binding site. Characterization of the binding behaviour shows the logical pattern of drugs as well as enlightening the elemental biochemical processes [55]. Molecular docking has been done to MBP3C using AUTODOCK 4.2 suite software. Way 2 drug predictive provides

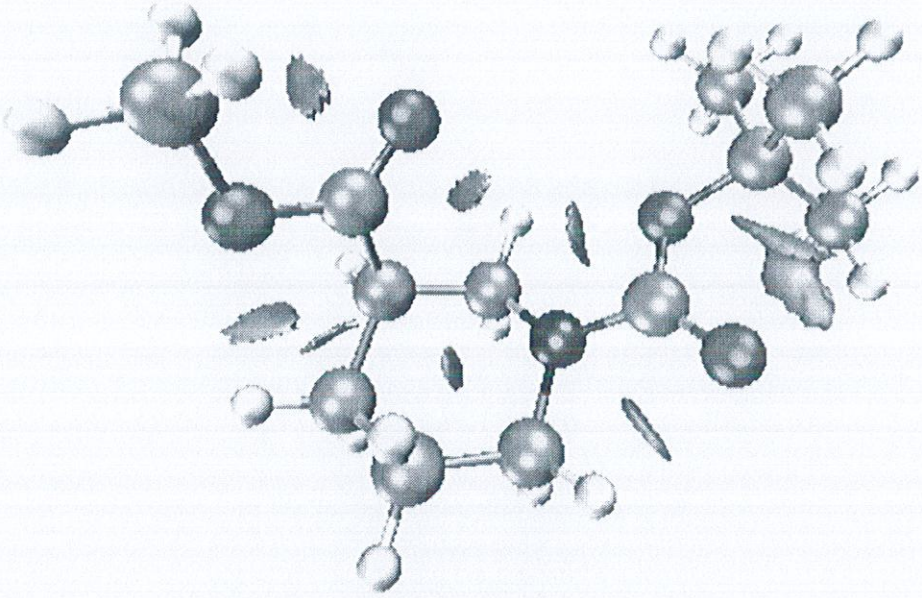

Fig. 8. a) RDG Isosurface of MBP3C, b) Scatter map of MBP3C.

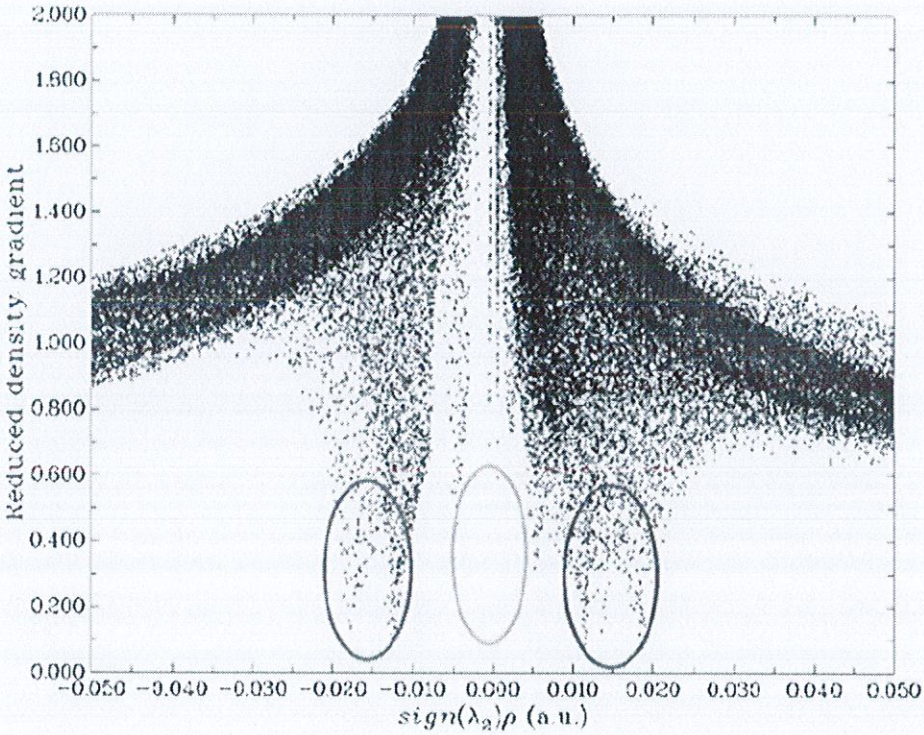

Fig. 8 (*continued*)

Table 9
Frequently considered drug likeness parameters.

Descriptor	MBP3C	Lipinski Rule
Hydrogen Bond Donor (HBD)	0	<5
Hydrogen Bond Acceptor (HBA)	4	<10
Topological polar surface area (TPSA) [Å^2]	55.84	<140
Molar refractivity	67.49	40 – 130
Log Kp(skin permeation)	−6.75 cm/s	
Number of rotatable bonds	5	<10
Bioavailability Score	0.55	

the knowledge of the biological property of MBP3C based on its structure. Proteins 5RH0,6Y9B and 2ACE were downloaded from protein bank (RCSB) belong to nootropic activity. Water molecules of the protein were removed, hydrogen and Kollman charges were added to the protein and were docked with the ligand. The inhibition constants (mM), molecular docking binding energies (kcal/mol), bond length(Å), number of hydrogen bonds and internal energies(kcal/mol) were obtained and shown in Table 11. Comparing the binding energy of the proteins with the ligand, 2ACE has the lowest binding energy −4.73 kcal/mol. This protein has two

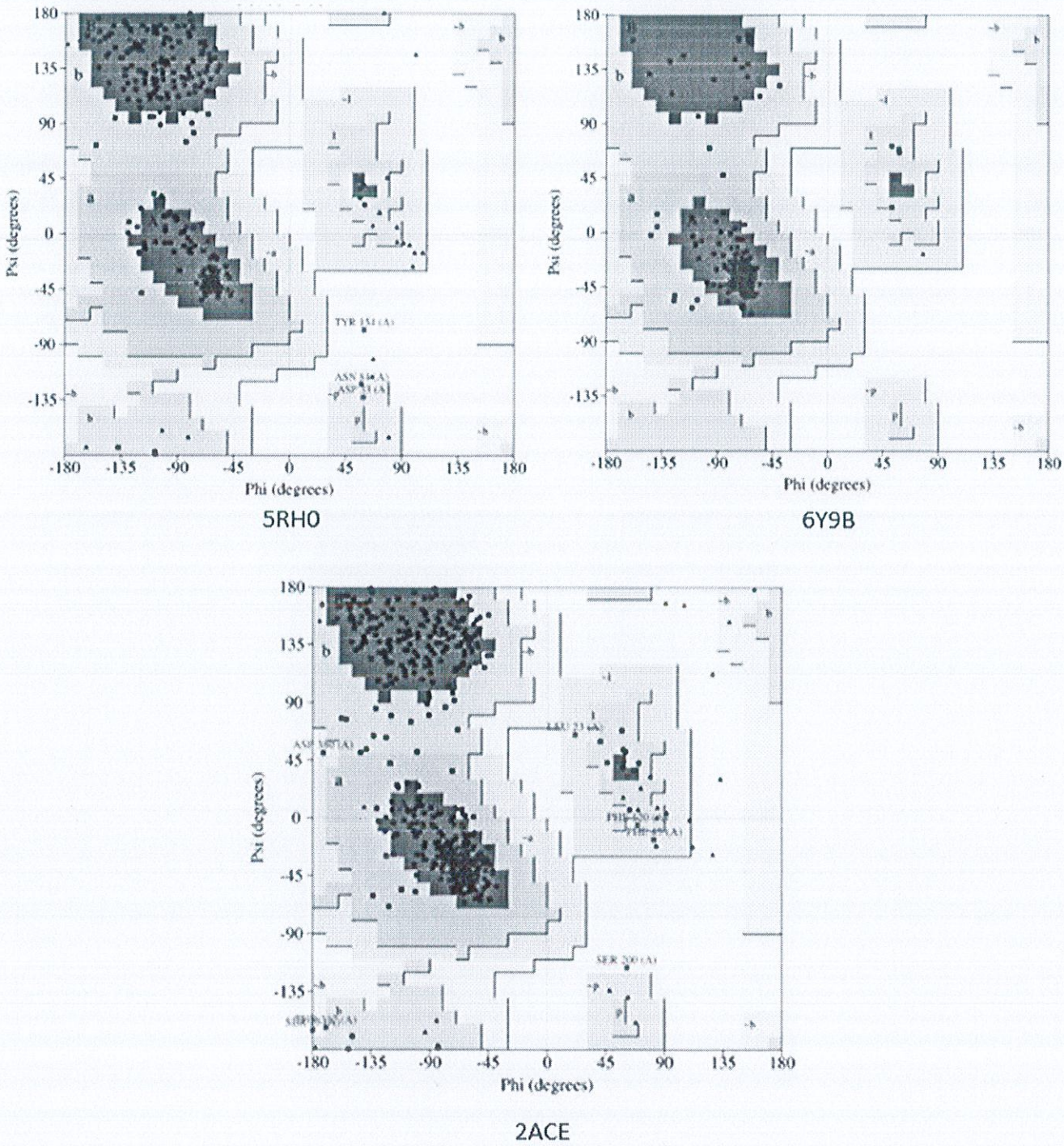

Fig. 9. Ramachandra plot for the proteins.

hydrogen bonds of length 3.5(Å) and 3.2(Å). The bonded residues of 2ACE to the ligand were TYR 121 and SER 122. The MBP3C ligand interaction with different receptors are shown in Fig. 10.

4. Conclusion

The entire calculations on Methyl N-Boc-piperidine-3-carboxylate (MBP3C) were carried out. Geometric parameters (bond angle, bond length) were computed and C_8–H_{22} has the shortest bond length. The topological properties such as electron density and Laplacian of the electron density helped to identify the closed as well as shared shell interactions between the intramolecular bonds present in the molecule. The energy gap, chemical softness and hardness of MBP3C in the gas phase and solvent phase are obtained from the frontier molecular analysis. Natural bond Analysis revealed that LP1(N5) participates as the donor and the σ* (O4–C12) anti bond as an acceptor [LP1(N5) → σ*(O4–C12)] with large stabilization energy 57.33 kcal/mol. Reactive sites were exposed in Molecular Electrostatic potential mapping and water possesses the highest

Table 10
Distribution of residues in the proteins.

Protein	Procheck parameters			
	most favoured region	additional allowed region	generally allowed region	disallowed region
5RH0	89%	9.90%	0.80%	0.40%
6Y9B	92.30%	7.70%	0%	0%
2ACE	87.30%	11.20%	1.30%	0.20%

Table 11
Hydrogen bonding and molecular docking of MBP3C .

protein	Bonded residues	No.of hydrogen bonds	Bond length (Å)	Binding energy (kcal/mol)	Inhibition constant (millimolar)	RMSD (A)	Internal energy (kcal/mol)
5RH0	GLN 299 ARG 298	2	3.3 3.1	−2.87	7.85	27.971	−3.36
6Y9B	LYS 116	1	3.5	−3.28	3.93	274.274	−4.54
2ACE	TYR 121 SER 122	2	3.5 3.2	−4.22	800.33 μM	75.905	−4.97

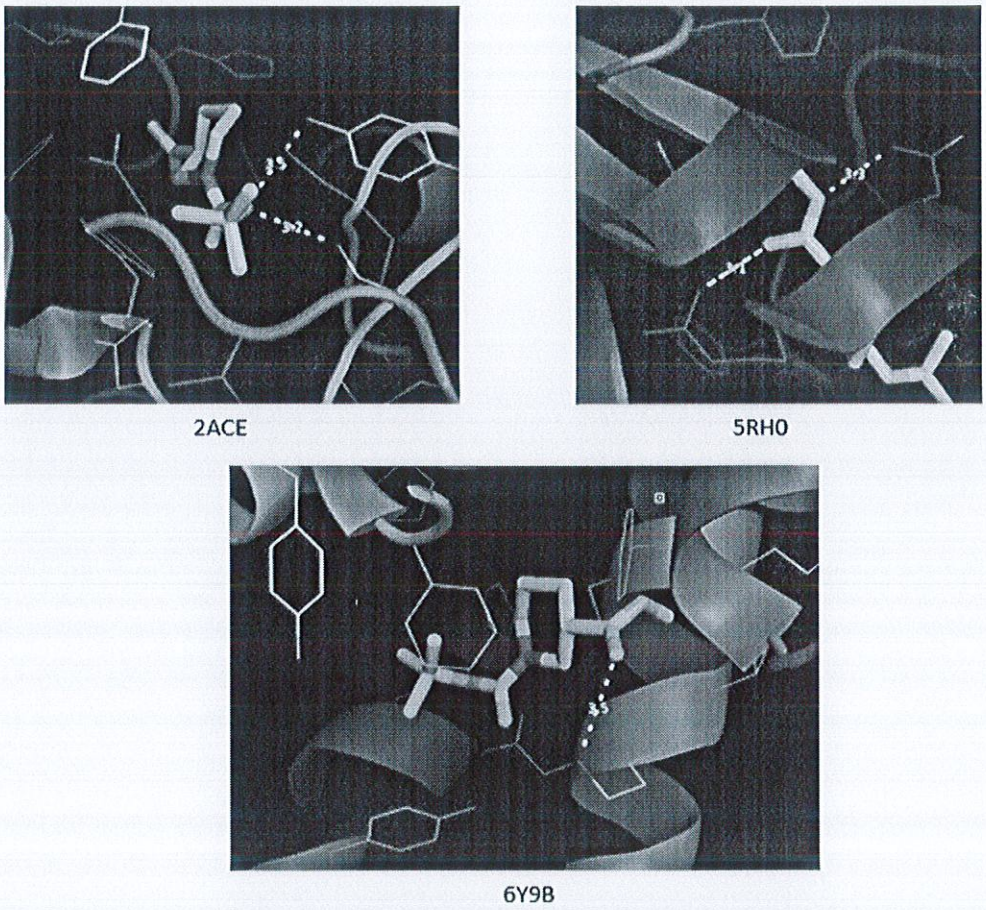

Fig. 10. Docking and Hydrogen bond interactions of MBP3C.

electrostatic potential. From the hyperpolarizability analysis, MBP3C was found to have large hyperpolarizability and water has 1.67 times higher polarizability than urea. DOS spectrum showed the electronic transition and bandgap energy values are determined in the gas phase as well as in the solvent phase. ELF and LOL have shown the localized bond around hydrogen atoms of MB3P. In all solvent analyses, the water showed the better change. NCI analysis showed the weak interaction area and steric effect of MB3P. The docking analysis was carried out for the title compound MBP3C and it showed the lowest

binding energy −4.73 kcal/mol with the protein 2ACE belongs to Nootropic activity.

CRediT authorship contribution statement

M. Vimala: Validation, Visualization, Writing – original draft, Writing – review & editing. **S. Stella Mary:** Conceptualization, Data curation, Formal analysis, Funding acquisition, Investigation. **R. Ramalakshmi:** Methodology, Project administration. **S. Muthu:** Supervision, Validation. **R. Niranjana Devi:** Project administration, Resources. **Ahmad Irfan:** Software, Visualization, Resources.

Declaration of Competing Interest

The authors declare that they have no known competing financial interests or personal relationships that could have appeared to influence the work reported in this paper.

Acknowledgements

We extend appreciation to the Deanship of Scientific Research at King Khalid University (KKU), Saudi Arabia for funding through research groups program under grant number R.G.P.1/16/42.

References

[1] Frank Johnson Welcher, Organic Analytical Reagents, volume3, Newyork (1947)..
[2] Senning, Alexander, Elsevier's Dictionary of Chemoetymology. Amsterdam, (2006)..
[3] E. Späth, G. Englaender, Über das Vor-kommen von Piperidin im schwarzen Pfeffer. Berichte Der Deutschen Chemischen Gesellschaft (A and B Series), 68 (12), (1935), 2218–2221. doi:10.1002/cber.19350681211..
[4] Kane, Vinayak , Jones, Maitland, "Spiro[5.7]trideca-1,4-dien-3-one",Organic Syntheses Collective, Volume, 7, (1990). doi:10.1002/0471264180.os061.27.
[5] A. Pianaro, E.G.P. Fox, O.C. Bueno, A.J. Marsaioli, Rapid configuration analysis of the solenopsins, Tetrahedron Asymmetry 23 (9) (2012) 635–642, https://doi.org/10.1016/j.tetasy.2012.05.0 05.
[6] Smith, Michael, March, Jerry, March's Advanced Organic Chemistry: Reactions, Mechanisms, and Structure (5th ed.). Wiley-Interscience, New York (2001)..
[7] E. Vitaku, D.T. Smith, J.T. Njardarson, Analysis of the Structural Diversity, Substitution Patterns and Frequency of Nitrogen Heterocycles among U.S. FDA Approved Pharmaceuticals, Journal of Medicinal Chemistry 57 (24) (2014) 10257–10274, https://doi.org/10.1021/jm501100b.
[8] N.E. Rogers, M.R. Avram, Medical treatments for male and female pattern hair loss, Journal of the American Academy of Dermatology 59 (4) (2008) 547–566, https://doi.org/10.1016/j.jaad.2008.07.001.
[9] Priscilla Kincaid-Smith, Vasodilators in the treatment of hypertension, J. Aust, Special Suppl. 1 (1975) 7–9, https://doi.org/10.5694/j.1326-5377. 1975.tb140363.x.
[10] M.A. Schuckit, Recognition and Management of Withdrawal Delirium (Delirium Tremens), New England Journal of Medicine 371 (22) (2014) 2109–2113.
[11] Stephen B. Hanauer, The role of loperamide in gastrointestinal disorders, Rev Gastroenterol Disord (2008) 15–20, PMID: 18477966.
[12] M. Negi, P.A. Chawla, A. Faruk, V. Chawla, Role of heterocyclic compounds in SARS and SARS CoV-2 pandemic, Bioorganic Chemistry (2020).
[13] A. Sagaama, O. Noureddine, Brandan SA, J.edryka AJ-, Flakus HT, Ghalla H, Issaoui N, Molecular docking studies, structural and spectroscopic properties of monomeric and dimeric species of benzofuran-carboxylic acids derivatives: DFT calculations and biological activities, Computational Biology and Chemistry (2020). doi: https:// doi.org/10.1016/j.compbiolchem.2020.107311..
[14] F. Akman, N. Issaoui, & A. S. Kazachenko, Intermolecular hydrogen bond interactions in the thiourea/water complexes (Thio-(H2O)n) (n = 1, . . ., 5): X-ray, DFT, NBO, AIM, and RDG analyses. Journal of Molecular Modeling, 26(6). (2020). doi:10.1007/s00894-020-04423-3..
[15] A. Sagaama, N. Issaoui, Design, molecular docking analysis of an anti-inflammatory drug, computational analysis and intermolecular interactions energy studies of 1-benzothiophene-2-carboxylic acid, Computational Biology and Chemistry 88 (2020), https://doi.org/10.1016/j.compbiolchem.2020.
[16] T.B. Issa, A. Sagaama, I. Noureddine, Computational study of 3-thiophene acetic acid: Molecular docking, electronic and intermolecular interactions investigations, Computational Biology and Chemistry 107268 (2020), https://doi.org/10.1016/j. compbiol chem.2020.10726.
[17] Davide Romani, Olfa Noureddine, Noureddine Issaoui, Silvia Brandán, Properties and Reactivities of Niclosamide in Different Media, a Potential Antiviral to Treatment of COVID-19 by Using DFT Calculations and Molecular Docking, Biointerface Research in Applied Chemistry, (2020).
[18] M. Frisch, G. Trucks, H. Schlegel, G. Scuseria, M. Robb, J. Cheeseman,G. Scalmani, V. Barone, B. Mennucci, G. Petersson, D. Daniels, O. Farkas, J. B. Foresman, J. V. Ortiz, J. Cioslowski, D. J. Fox., Gaussian 09, Revision D.01, Gaussian Inc., Wallingford (CT), (2013).
[19] T.K .Roy Dennington and J.M. GaussView, Version 5, Semichem Inc, Shawnee Mission KS, 2009. http://www.gaussian.com/g_tech/gv5ref/gv5citation.htm..
[20] J. Chocholoušová, V. Špirko, P. Hobza, First local minimum of the formic acid dimer exhibits simultaneously red-shifted O-H···O and improper blue-shifted C–H···O hydrogen bonds, Phys. Chem. Chem. Phys. 6 (1) (2004) 37–41, https://doi.org/10.1039/b314148a.
[21] T.A.Keith, T.K.Gristmill Software, Overland Park KS, AIMALL(Version 11.05.16), 2011.
[22] T. Lu, F. Chen, Multiwfn: A multifunctional wavefunction analyzer, Journal of Computational Chemistry 33 (5) (2011) 580–592, https://doi.org/10.1002/jcc.22885.
[23] N. M. O'Boyle, A. L. Tenderholt and K. M. Langner. A Library for Package-Independent Computational Chemistry Algorithms. Journal of Computational Chemistry,29, (2008), 839-845.http://dx.doi.org/10.1002/jcc.20823J..
[24] G.M. Morris, R. Huey, W. Lindstrom, M.F. Sanner, R.K. Belew, D.S. Goodsell, A.J. Olson, Autodock4 and AutoDockTools4: automated docking with selective receptor flexiblity, J. Computational Chemistry 2009 (2009) 2785–2791.
[25] Barton, Derek, "The Principles of Conformational Analysis". Nobel Media AB 2013.Elsevier Publishing Co. 169 (3945), (1970) 539- 544. doi: 10.1126/science.16 9.3945. 539.
[26] H.-K.Fun, S.Arshad, S. Dinesh, S.Vivek,& G. K. Nagaraja, 1-(tert-Butoxycarbonyl) piperidine-4-carboxylic acid. Acta Crystallographica Section E Structure Reports Online, 67(9), (2011) 2215–2215. doi:10.1107/s1600536811030145..
[27] F. Weinhold, C.R. Landis, Natural bond orbitals and extensions of localized bonding concepts, Chem. Educ. Res. Pract. 2 (2) (2001) 91–104, https://doi.org/10.1039/b1rp90011k.
[28] N. Issaoui, N. Rekik, B. Oujia, M.J. Wójcik, Theoretical infrared line shapes of H-bonds within the strong anharmonic coupling theory and Fermi resonances effects, International Journal of Quantum Chemistry 110(14)(2010)2583–2602.
[29] S.S. Khemalapure, V.S. Katti, C.S. Hiremath, S.M. Hiremath, M. Basanagouda, S. B. Radder, Spectroscopic (FT-IR, FT-Raman, NMR and UV-Vis), ELF, LOL, NBO, and Fukui function investigations on (5-bromo-benzofuran-3-yl)-acetic acid hydrazide (5BBAH): Experimental and theoretical approach, Journal of Molecular Structure. (2019), https://doi.org/10.1016/j.molstruc.2019.06.078.
[30] R.F.W. Bader, Atoms in Molecules: A Quantum Theory, Oxford Univ, Press, 1990.
[31] J. Kozisek, N.K. Hansen, H. Fuess, Acta Cryst. B 58 (2002) 463–470.
[32] N. Rekik, N. Issaoui, B. Oujia, M.J. Wójcik, Theoretical IR spectral density of H-bond in liquid phase: Combined effects of anharmonicities, Fermi resonances, direct and indirect relaxations, Journal of Molecular Liquids 141 (3) (2008) 104–109.
[33] N. Issaoui, N. Rekik, B. Oujia, M.J. Wójcik, Anharmonic effects on theoretical IR line shapes of medium strong H(D) bonds, International Journal of Quantum Chemistry 109 (3) (2009) 483–499, https://doi.org/10.1002/qua.21839.
[34] J.S. Murry, K. Sen, Molecular electrostatic potential: concepts and applications, Elsevier, Amesterdam, 1996.
[35] A. Matondo, R. Thomas, P.V. Tsalu, C.T. Mukeba, V. Mudogo, α-methylation and α-fluorination electronic effects on the regioselectivity of carbonyl groups of uracil by H and triel bonds in the interaction of U, T and 5FU with HCl and TrH3 (Tr= B, Al), J. Mol. Graph. Model. 88 (2019) 237–246.
[36] J. Daintith, A Dictionary of Chemistry, 7th edition, New York, (2004)..
[37] J.S. Griffith, L.E. Orgel, Ligand-field theory, Quarterly Reviews, Chemical Society 11 (4) (1957) 381–393, https://doi.org/10.1039/qr9571100381.
[38] Onkar Prasad, Leena Sinha, and Naveen Kumar, Theoretical Raman and IR spectra of tegafur and comparison of molecular electrostatic potential surfaces, polarizability and hyerpolarizability of tegafur with 5-fluoro-uracil by density functional theory, J. At. Mol. Sci, Vol. 1, No. 3, (2010), 201-214. doi: 10.4208/jams.032510.042010a.
[39] Y.S. Priya, K.R. Rao, P.V. Chalapathi, A. Veeraiah, K.E. Srikanth, Y.S. Mary, R. Thomas, Intricate spectroscopic profiling, light harvesting studies and other quantum mechanical properties of 3-phenyl-5-isooxazolone using experimental and computational strategies, J. Mol. Struct. 1203 (2020), https://doi.org/10.1016/j.molstruc.2019.127461.
[40] F. Mendez, J.L. Gazquez, Chemical Reactivity of Enolate Ions: The Local Hard and Soft Acids and Bases Principle Viewpoint, Journal of the American Chemical Society 116 (20) (1994) 9298–9301, https://doi.org/10.1021/ja00099a055.
[41] P.K. Chattaraj, B. Maiti, U. Sarkar, Philicity, A Unified Treatment of Chemical Reactivity and Selectivity, The Journal of Physical Chemistry A 107 (25) (2003) 4973–4975, https://doi.org/10.1021/jp034707u.
[42] C. Karnan, A.R. Prabakaran, Investigation on new NLO material L-histidine potassium pentaborate (LHKB5), International Journal of Scientific Research in Physics and Applied Sciences 7 (1) (2019) 46–51, https://doi.org/10.26438/ijsrpas/v7i1.4651.
[43] G.A. DiLabio, P.G. Piva, P. Kruse, R.A. Wolkow, Dispersion Interactions Enable the Self-Directed Growth of Linear Alkane Nanostructures Covalently Bound to Silicon, Journal of the American Chemical Society 126 (49) (2004) 16048–16050, https://doi.org/10.1021/ja0460007.
[44] B. Silvi, A. Savin, Classification of chemical bonds based on topological analysis of electron localization functions, Nature 371 (6499) (1994) 683–686, https://doi.org/10.1038/371683a0.

[45] H. Jacobsen, Localized-orbital locator (LOL) profiles of chemical bonding, Canadian Journal of Chemistry 86 (7) (2008) 695–702, https://doi.org/10.1139/v08-052.
[46] S.N. Steinmann, Y. Mo, C. Corminboeuf, How do electron localization functions describe π-electron delocalization?, Physical Chemistry Chemical Physics 13 (46) (2011) 20584–20592, https://doi.org/10.1039/c1cp21055f.
[47] H. Fenniri, P. Mathivanan, K.L. Vidale, D.M. Sherman, K. Hallenga, K.V. Wood, J. G. Stowell, Helical Rosette Nanotubes: Design, Self-Assembly, and Characterization, Journal of the American Chemical Society 123 (16) (2001) 3854–3855, https://doi.org/10.1021/ja005886l.
[48] C.A. Lipinski, Lead-and drug-like compounds: the rule-of-five revolution, Drug Discov. Today Technol. 1 (4) (2004) 337e341.
[49] A. Daina, O. Michielin, V. Zoete, iLOGP: A Simple, Robust, and Efficient Description of n-Octanol/Water Partition Coefficient for Drug Design Using the GB/SA Approach, Journal of Chemical Information and Modeling 54 (12) (2014) 3284–3301, https://doi.org/10.1021/ci500467k.
[50] S.C. Lovell, I.W. Davis, W.B. Arendall, P.I.W. de Bakker, J.M. Word, M.G. Prisant, D.C. Richardson, Structure validation by Cα geometry: ϕ, ψ and Cβ deviation, Proteins: Structure, Function, and Bioinformatics 50 (3) (2003) 437–450, https://doi.org/10.1002/prot.10286.
[51] M.L. Raves, M. Harel, Y.-P. Pang, I. Silman, A.P. Kozikowski, J.L. Sussman, Structure of acetylcholinesterase complexed with the nootropic alkaloid, (−)-huperzine A, Nature Structural & Molecular Biolog, y 4 (1) (1997) 57–63, https://doi.org/10.1038/nsb0197-57.
[52] A.S. Godoy, N.C.M.R. Mesquita, Oliva, G, PanDDA analysis group deposition – Crystal Structure of Zika virus NS3 Helicase in complex with Z1444783243, DOI: 10.2210/pdb5RHO/pdb..
[53] W. Oosterheert & P. Gros, Cryo-EM structure and potential enzymatic function of human six-transmembrane epithelial antigen of the prostate 1. Journal of Biological Chemistry, jbc.RA120.013690. (2020). doi:10.1074/jbc.ra120.013690.
[54] B. Douglas Kitchen, R. Hélène Decornez, John Furr, Jürgen Bajorath, Docking and scoring in virtual screening for drug discovery: methods and applications, Nature Reviews Drug Discovery 3 (2004) 935–949, https://doi.org/10.1038/nrd1549.
[55] S. Christopher Jeyaseelan, A. Milton Franklin Benial, Spectroscopic characterization, DFT studies, molecular docking and cytotoxic evaluation of 4-nitro-indole-3-carboxaldehyde: A potent lung cancer agent, Journal of Molecular Recognition e2872 (2020), https://doi.org/10.1002/jmr.2872.

Registrar
St. Peter's Institute of Higher Education and Research
(Deemed to be University U/S 3 of the UGC Act, 1956)
Avadi, Chennai-600 054

St. Peter's Institute of Higher Education and Research
Deemed to be University
Chennai
600 054